VIP *Very Important Paper*

# C–H Amination via Nitrene Transfer Catalyzed by Mononuclear Non-Heme Iron-Dependent Enzymes

Maria Agustina Vila[+],[a] Viktoria Steck[+],[b] Sonia Rodriguez Giordano,[a] Ignacio Carrera,*[a] and Rudi Fasan*[b]

Expanding the reaction scope of natural metalloenzymes can provide new opportunities for biocatalysis. Mononuclear non-heme iron-dependent enzymes represent a large class of biological catalysts involved in the biosynthesis of natural products and catabolism of xenobiotics, among other processes. Here, we report that several members of this enzyme family, including Rieske dioxygenases as well as α-ketoglutarate-dependent dioxygenases and halogenases, are able to catalyze the intramolecular C–H amination of a sulfonyl azide substrate, thereby exhibiting a promiscuous nitrene transfer reactivity. One of these enzymes, naphthalene dioxygenase (NDO), was further engineered resulting in several active site variants that function as C–H aminases. Furthermore, this enzyme could be applied to execute this non-native transformation on a gram scale in a bioreactor, thus demonstrating its potential for synthetic applications. These studies highlight the functional versatility of non-heme iron-dependent enzymes and pave the way to their further investigation and development as promising biocatalysts for non-native metal-catalyzed transformations.

Mononuclear non-heme iron (NHI) enzymes participate in a broad range of oxidative processes implicated in the biosynthesis of antibiotics and other natural products, DNA repair mechanisms, and the metabolic degradation of xenobiotics.[1] As part of their native function, these enzymes catalyze a variety of oxidation reactions mediated by high-valent iron-oxo intermediates, including C($sp^3$)–H hydroxylation and halogenation via H-atom abstraction/radical rebound, desaturation, and arene hydroxylation and dihydroxylation reactions.[2] The specific reactivity of these enzymes is influenced by the first and second sphere coordination environment around the catalytic iron center in the active site (Figure 1). Rieske dioxygenases are multicomponent enzymes usually comprising two or three component systems: a reductase that obtains electrons from NAD(P)H, often a Rieske ferredoxin component that transfers the electrons, and an oxygenase component that promotes the *cis*-1,2-dihydroxylation of arene substrates (e.g. naphthalene, toluene), among other reactions.[1j,3] The oxygenase unit consist of a catalytic α subunit and a structural β subunit organized into an $\alpha_3\beta_3$ complex, where the active site iron atom is coordinated by a '2-His-1-carboxylate facial triad' composed of two His residues and a carboxylate group from an Asp or Glu residue in the protein, along with one or two water molecules (Figure 1A).[4] The iron center is linked to a proximal [2Fe-2S] cluster via a conserved aspartate hydrogen-bonded to the metal-coordinating histidine ligands, which facilitates transfer of electrons during catalysis.[3] While featuring a similar 2-His-1-carboxylate-bound iron center, members of the large subclass of α-ketoglutarate (αKG)-dependent dioxygenases utilize αKG as the source of electrons and co-substrate for oxidation (Figure 1B).[1i,5] In these enzymes, αKG participates in the coordination of the Fe(II) atom prior to catalysis and hydroxylation of the substrate is accompanied by oxidation of αKG to $CO_2$ and succinate. In αKG-dependent halogenases, the carboxylate ligand is missing, resulting in a vacant coordination site that accommodates a halide ligand (i.e., $Cl^-$ or $Br^-$; Figure 1C).[6] During catalysis, this allows for the transfer of a halide radical to the carbon radical generated upon H-atom abstraction in the substrate from the iron(IV)-oxo intermediate, resulting in a C($sp^3$)–H chlorination (or bromination) reaction. While these enzymes have been extensively investigated in the context of their native reactions,[7] their potential reactivity toward non-native transformations has remained largely unexplored.[8]

Recently, the Rieske toluene dioxygenase (TDO) from *Pseudomonas putida* F1 was found to catalyze an unexpected transformation resulting in the conversion of benzyl azide to benzonitrile, in addition to the expected *cis*-dihydroxylation product (Figure 2A). Based on computational (DFT) and mechanistic studies, we proposed a plausible mechanism for this reaction that involves the formation of an iron(IV)–nitrene intermediate, which, upon rearrangement of the hydroxyl group and dehydration of the resulting benzaldoxime, leads to the observed benzonitrile product.[9] A similar activity was subsequently observed for Fe/αKG-dependent dioxygenases.[10] Interestingly, the proposed mechanism for these reactions shares similarities with that reported for the P450- and Mb-catalyzed oxidative deamination of benzyl azides to yield

[a] Dr. M. A. Vila,[+] Prof. Dr. S. Rodriguez Giordano, Prof. Dr. I. Carrera
Laboratorio de Biocatálisis y Biotransformaciones, Departamento de Química Orgánica y Departamento de Biociencias. Facultad de Química
Universidad de la República
Av General Flores 2124, CP 11800 Montevideo (Uruguay)
E-mail: icarrera@fq.edu.uy
[b] Dr. V. Steck,[+] Prof. Dr. R. Fasan
Department of Chemistry
University of Rochester
RC Box 270216, Rochester, NY 14627 (USA)
E-mail: rfasan@ur.rochester.edu
[+] These authors contributed equally to this manuscript

Supporting information for this article is available on the WWW under https://doi.org/10.1002/cbic.201900783

*This article is part of a Special Collection on Xenobiology. To view the complete collection, visit our homepage*

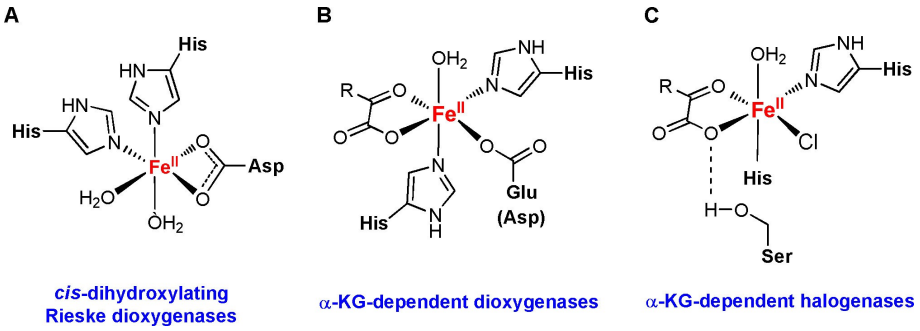


**Figure 1.** Active sites of the different classes of mononuclear non-heme iron (NHI) enzymes investigated in this work: (**A**) Rieske dioxygenases; (**B**) α-ketoglutarate-dependent dioxygenases; (**C**) α-ketoglutarate-dependent halogenases.

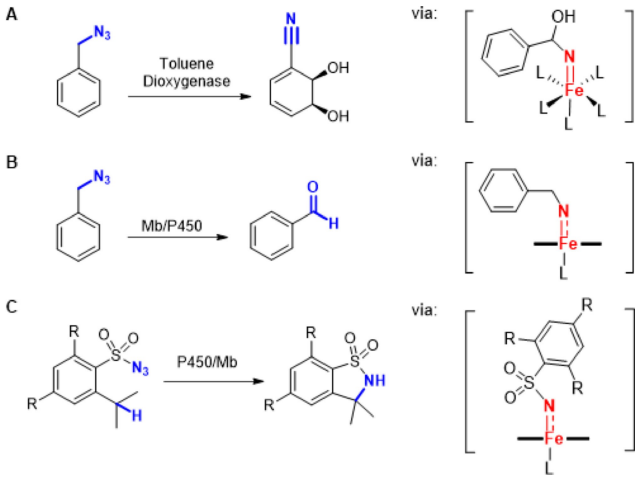


**Figure 2.** Enzyme-catalyzed transformations involving iron nitrene species: (**A**) TDO-catalyzed conversion of benzyl azide to benzonitrile and subsequent dihydroxylation; (**B**) Mb/P450-catalyzed oxidative deamination of benzyl azides; (**C**) P450/Mb-catalyzed C–H amination of sulfonyl azides.

benzaldehydes (Figure 2B).[11] In addition, the putative iron–nitrene intermediate invoked in the context of the TDO reaction is analogous to that previously proposed by us to mediate C–H amination reactions via nitrene transfer supported by engineered P450 s[12] or other hemoproteins (Figure 2C).[13] Based on these considerations, we surmised that Rieske dioxygenases and potentially other non-heme iron enzymes could be able to exhibit non-native nitrene transfer reactivity.

To test this hypothesis, we surveyed a diverse panel of functionally and structurally different non-heme iron-dependent oxidases. This enzyme selection included the Rieske toluene (TDO), chlorobenzene (CBDO) and naphthalene (NDO) dioxygenases, which catalyze the *cis*-dihydroxylation of the corresponding aromatic compound. TDO, which accepts a wide variety of mono and disubstituted arenes as substrates, has been extensively used in the last decades as a whole cell biocatalyst for the preparation of enantiopure *cis*-cyclohexadienediols for enantioselective synthesis.[14] In contrast, NDO engages larger substrates such as polycyclic arenes,[15] while the substrate scope of CBDO has been much less explored.[16] Additionally, the enzyme panel included representative members of the subclass of Fe/αKG-dependent dioxygenases, namely *E. coli* taurine dioxygenase TauD, which catalyzes the oxidation of 2-aminoethanesulfonic acid (taurine) under sulfur starvation conditions[17] and tolerates non-native substrates;[17b] *E. coli* AlkB, which is involved in the repair of alkylated DNA;[1a,18] *E. coli* Gab dioxygenase, a clavaminate synthase-like enzyme putatively involved in the biosynthesis of β-lactam secondary metabolites;[19] the multifunctional fungal dioxygenase AsqJ (*Aspergillus nidulans*), which catalyzes a tandem desaturation/epoxidation reaction during the biosynthesis of the alkaloid 4′-methoxyviridicatin;[1d,20] and the plant hyoscyamine 6β-hydroxylase (H6H), which catalyzes a hydroxylation/dehydrogenation/epoxidation sequence in the biosynthesis of the anticholinergic alkaloid scopolamine in the Solanaceae family of plants.[21] As a representative member of NHI halogenases, we included in the panel the cyanobacterial enzyme WelO5, which catalyzes the chlorination of 12-epi-fischerindole as part of the biosynthesis of the welwitindolinone natural products.[22] Compared to other well characterized NHI halogenases such as SyrB2,[23] WelO5 was chosen because it acts on a free-standing small-molecule substrate as opposed to a carrier protein-linked substrate. In addition, its structure was recently elucidated by X-ray crystallography.[22c]

Starting with the Rieske dioxygenases, we tested these enzymes for their C–H amination activity using as a model reaction the conversion of 2,4,6-triisopropylbenzenesulfonyl azide **1a** to the sultam product **1b** (Figure 3A). Due to the multicomponent nature of Rieske dioxygenases, NDO, TDO and CBDO were expressed in *E. coli* strains and tested in whole-cell biotransformations.[24] Initial tests revealed that all of these Rieske enzymes biocatalysts exhibited detectable C–H amination activity (see Table S1 in the Supporting Information). Based on these promising results, the reaction conditions for these biotransformations were further optimized (see Figures S1 in the Supporting Information). Under optimized conditions, both NDO and CBDO were found to provide a significantly higher conversion of sulfonyl azide **1a** to the C–H amination product **1b** compared to the control strains (37–38% vs. 20–22%; Figure 3B). The observed background activity may stem from heme-containing enzymes present in *E. coli*.[25] For the NDO-expressing cells, further improved conversion of **1a** into **1b** over the background levels was achieved at higher substrate

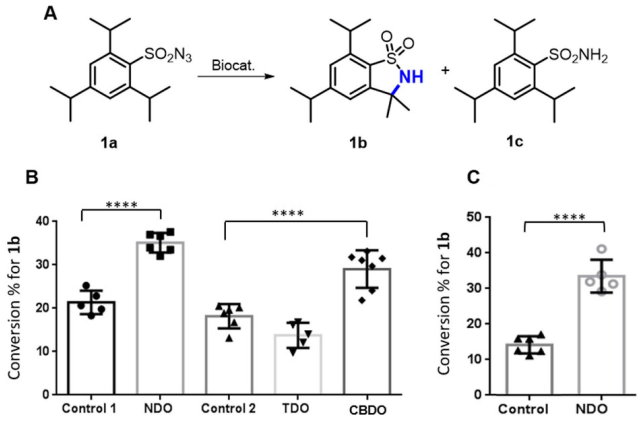


**Figure 3.** C–H amination of 2,4,6-triisopropylbenzenesulfonyl azide **1a** with Rieske dioxygenases (A). (B) Biotransformations with **1a** (5 mM) using *E. coli* whole cells expressing NDO (JM109(DE3) (pDTG141)); TDO (JM109 (pDTG601)); CBDO (JM109 (pKK-CBDO)) at $OD_{600} = 60$ in potassium phosphate buffer (50 mM, pH 7.2), anaerobic conditions. Control 1: *E. coli* JM109 (DE3). Control 2: *E. coli* JM109 (pKK223-3). In each case, sulfonamide (**1c**) amounted to < 5%. (C) Same reaction of NDO and control as in (B) but with 10 mM **1a**.

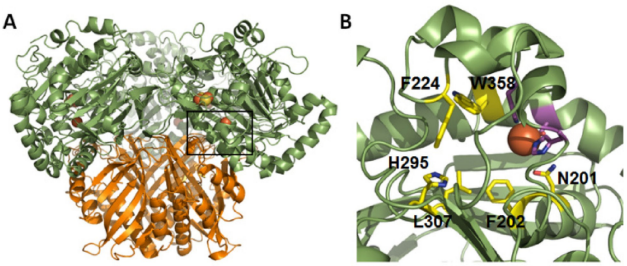


**Figure 4.** NDO structure (pdb 1NDO). (**A**) Quaternary structure ($\alpha_3\beta_3$) of NDO showing alpha subunits in green and beta subunits in orange. (**B**) View of the active site (boxed panel (A)) showing the iron atom (red, sphere), Fe-coordinating residues (purple, stick) and active site residues targeted for mutagenesis (yellow, stick model).

loading (i.e. 10 mM vs. 5 mM, Figure 3C). In contrast to NDO and CBDO, the cells expressing TDO showed no significant activity over background levels (Figure 3B). Overall, these results demonstrate for the first time that the NDO and CBDO Rieske dioxygenases possess promiscuous nitrene transferase activity that can be applied for catalyzing C–H amination reactions. Along with the C–H amination product, both biocatalysts were found to generate a small amount of sulfonamide **1c** (approx. 4%). This by-product was previously observed also in the context of hemoprotein-catalyzed nitrene transfer reactions with sulfonyl azides and other azide-based nitrene precursors.[12,26] Nevertheless, both Rieske enzymes showed a high selectivity toward the formation of the desired C–H amination product **1b** (> 90%) over this side reaction. Interestingly, the NDO-dependent C–H amination activity was found to be reasonably oxygen tolerant, maintaining in the presence of air approximately 60% of the activity levels observed under anaerobic conditions (see Figure S2 in the Supporting Information). This is in contrast to P450-catalyzed nitrene transfer reactions, which require strictly anaerobic conditions both with purified proteins and in whole cells.[12,26]

Encouraged by these findings, we selected NDO as the target for mutagenesis studies in order to gain insights into the effect of active site mutations on the non-native C–H amination activity of this enzyme. To this end, we generated a series of libraries sampling 12 representative amino acids with different side-chain groups–i.e., Phe, Ser, Tyr, Leu, Pro, His, Ile, Thr, Asn, Val, Ala, Asp, using the degenerate NHT codon–[27] at positions Asn201, Phe202, His295, Leu307, Phe352 and Trp358, which are located within the substrate binding pocket of the enzyme[28] (Figure 4). Since Phe224 serves as a gating residue at the entrance of the substrate channel leading to the active site,[29] this position was replaced with eight smaller amino acids (i.e., Ile, Thr, Asn, Ser, Val, Ala, Asp, Gly) using the RNC degenerate codon. These libraries were expressed in 48-well plates and screened for C–H amination activity toward substrate **1a** by HPLC. The initial screening experiments showed that mutagenesis of positions N201, F202 and F352 had mostly deleterious effects on the C–H amination activity of the enzyme. In contrast, various large-to-small mutations at positions Phe224 (→Ala, Ile, Val), His295 (→Ile, Thr, Val), and Trp358 (→Asn, along with Phe and Tyr) led to wild type-like activity toward the non-native reaction (see Figure S3 in the Supporting Information). At position 307, a Leu→His mutation was also tolerated.

Based on these results, the aforementioned mutations were recombined to generate a double and triple mutant library. From this library, NDO variants carrying a F224V mutation along with H295I, H295T, or H295V, were found to be functional C–H aminases (Figure S3). Although none of these NDO variants showed improved C–H amination activity compared to the wild-type enzyme, these results showed that mutation of various active site positions, and in particular at the level of residues 224, 295, 307, and 358, are compatible with this non-native reactivity, and expected to facilitate further protein engineering efforts.

In order to examine the synthetic potential of NDO in the context of this non-native reaction, we performed a large-scale biotransformation of **1a** (1 g, 3 mM) with NDO-expressing *E. coli* JM109 (DE3) cells in a bioreactor (5 L). For this purpose, we used our previously optimized fed-batch protocol to express the dioxygenase in a high cell density culture (approx. 50 g/L cdw), where the substrate is added after reaching stationary phase.[30] As shown in Figure 5, this experiment showed progressive consumption of the azide substrate **1a** and concomitant accumulation of the desired sultam product **1b** within three hours. Under these conditions, only a negligible fraction of the sulfonamide by-product **1c** was generated in the course of the reaction. Overall, this protocol enabled the conversion of 1 g **1a** into **1b** in 45% yield and > 90% selectivity, thus providing a proof-of-concept of the scalability of the NDO-driven reaction.

After the promising results obtained for the Rieske biocatalysts, we investigated the C–H amination activity of other NIH enzymes such as Fe/αKG-dependent dioxygenases and halogenases. As summarized in Table 1, all of the tested Fe/

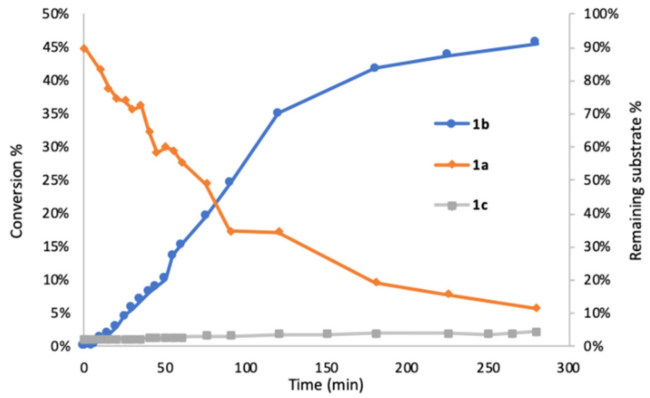


**Figure 5.** Biotransformation profile for the C–H amination reaction of 1 gram of 2,4,6-triisopropylbenzensulfonyl azide **1a** carried out in a 5 L bioreactor using *E. coli* JM109 (DE3) (pDTG141-Kan).

**Table 1.** Activity and selectivity of Fe/αKG-dependent dioxygenases and halogenases toward the intramolecular C–H amination of 2,4,6-triisopropylbenzensulfonyl azide **1a** (reaction (1)) and 2-phenylpropyl carbonazidate **2a** (reaction (2)).[a]

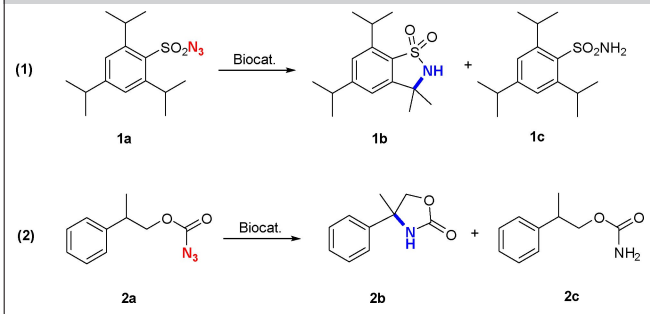


| Entry | Enzyme | Conditions[b] | 1b Yield[c] (Selectivity)[d] | 2b Yield[c] (Selectivity)[d] |
|---|---|---|---|---|
| 1 | TauD | A | 27% (63%) | n.a. |
| 2 | TauD | B | 13% (62%) | n.a. |
| 3 | AlkB | A | n.a. | 2% (30%) |
| 4 | AlkB | B | n.a. | n.a. |
| 5 | Gab | A | 14% (57%) | n.a. |
| 6 | Gab | B | 13% (53%) | n.a. |
| 7 | AsqJ | A | 24% (67%) | n.a. |
| 8 | AsqJ | B | 12% (59%) | n.a. |
| 9 | H6H | A | 13% (33%) | 6% (27%) |
| 10 | H6H | B | n.a. | n.a. |
| 11 | WelO5 | A | 15% (58%) | n.a. |
| 12 | WelO5 | B | 13% (61%) | 3% (80%) |

[a] *E. coli* cells expressing the indicated enzyme at $OD_{600}=40$ in 50 mM kPi buffer (pH 7.0), 3 mM substrate. Condition A: no additives; Condition B: containing aKG, ascorbate, and iron salt (Table S2). [c] HPLC yield as calculated based on calibration curve with authentic standards, and subtracted by the background activity of BL21 cells. N.a. = not active. [d] Selectivity for formation of C–H amination product over reduction (and alcohol) byproduct, i.e., **1b**/(**1b**+**1c**) or **2b**/(**2b**+**2c**+**2d**). See also Figures S5 and S6.

αKG-dependent dioxygenases and halogenases, with the only exception of AlkB, were found to display promiscuous C–H amination activity in the reaction with **1a**. Among them, TauD and AsqJ showed the highest activity, resulting in the generation of the C–H amination product in 25–27% yield as determined by HPLC. Since these enzymes rely on αKG as co-substrate for metal coordination in the context of their native dioxygenase / halogenase activity, these reactions were also carried out in the presence of media supplemented with αKG along with iron and ascorbic acid. Interestingly, a differential effect of the added αKG was observed for the different enzymes. Specifically, no change in C–H amination activity was observed for Gab and WelO5 under these conditions, whereas an approximately 2-fold reduction in yield was noted for TauD, AsqJ and H6H. These results suggest that at least for the latter enzymes, αKG may not be required and possibly has an inhibitory effect in the context of the non-native reaction. For most of the active enzymes, the C–H amination was found to proceed with relatively good selectivity, ranging from 53 to 67%. As an exception, H6H exhibited modest chemoselectivity (33%), producing sulfonamide **1c** as the major product of the reaction.

These experiments thus demonstrated that both Rieske and Fe/αKG-dependent dioxygenases/halogenases possess promiscuous nitrene transferase activity. On the basis of these results, the entire enzyme panel was further tested for their ability to catalyze another type of intramolecular C–H amination reaction, namely the cyclization of carbonazidate **2a** to give the oxazolidinone product **2b** (Table 1).[12b] While Rieske dioxygenases did not show detectable activity toward this substrate (data not shown), some of the Fe/αKG-dependent enzymes exhibited appreciable activity toward this nitrene transfer reaction. In particular, the dioxygenases AlkB and H6H and chlorinase WelO5 were found able to covert **2a** into **2b** in 2–6% yield in the whole-cell reactions. Furthermore, while AlkB and H6H were found to produce 2-phenylpropyl carbamate (**2c**) as well as 2-phenylpropan-1-ol (**2d**) as byproducts, the latter being observed also in the context of the P450-catalyzed reaction,[12b] WelO5 exhibited a significantly higher selectivity for the desired C–H amination reaction, producing **2b** with 80% selectivity and no alcohol byproduct (Table 1, Entry 12; SI Figure S6). Altogether, these experiments revealed that NHI enzymes are able to engage different types of nitrene donors in intramolecular C–H amination reactions, with the individual members of this group displaying differential selectivity and reactivity toward the two different azide substrates. While the mechanism of these reactions awaits further elucidation, our previous studies[9,11] suggest a mechanism analogous to that of hemoprotein-catalyzed C–H amination,[12–13] in which binding of the azide substrate to the iron center leads to an iron-nitrene intermediate via nitrogen extrusion, followed by a nitrene C–H insertion process.

In summary, this work demonstrates that mononuclear non-heme iron-dependent oxidases are capable of catalyzing intramolecular C–H amination reactions involving sulfonyl azides and carbonyl azides, thereby exhibiting a promiscuous nitrene transferase activity. While this work was being finalized for submission, the Arnold group reported a similar type of reactivity for the Fe/αKG-dependent *Pseudomonas savastanoi* ethylene-forming enzyme (PsEFE).[31] Complementing and expanding upon these findings, the present studies show that other types of αKG-dependent dioxygenases as well as Rieske

dioxygenases and αKG-dependent halogenases exhibit such non-native reactivity. Through mutagenesis studies, we gained initial insights into the tolerance of active site mutations within the Rieske naphthalene dioxygenase NDO toward this catalytic activity. Notably, this enzyme could be applied for a gram-scale C–H amination reaction in a bioreactor, which provides a proof-of-principle demonstration of its synthetic potential in the context of this non-native transformation. Overall, our studies illustrate the functional versatility of non-heme iron-dependent enzymes and open the way to their further investigation and development as biocatalysts for other non-native metal-catalyzed transformations, which are the subject of ongoing studies in our laboratory.

## Experimental Section

### Reagents and analytical methods

Chemical reagents and solvents were purchased from Sigma-Aldrich unless otherwise stated. Compound 1a, 1b, 2a, 2b, 1c and 2cwere prepared as reported previously.[12] HPLC analyses were performed using a Shimadzu LC-2010A-HAT equipped with a VisionHT-C18 reverse-phase column and a multi-diode UV-Vis detector, or on a Shimadzu Prominence Liquid Chromatograph LC-20AT equipped with an Eclipse XDB-C18 Zorbax reverse-phase column (250 mm length, 4.6 mm diameter, 5 μm particle size) and a diode-array detector.

### Strains and plasmids

*E. coli* JM109 were obtained from New England Biolabs and *E. coli* JM109 (DE3) from Promega. *E. coli* JM109 (pDTG601) expressing Toluene Dioxygenase (TDO) was kindly donated by Prof. David T. Gibson, *E. coli* JM109 (DE3) (pDTG141) expressing Naphthalene Dioxygenase (NDO) was obtained from Prof. Rebecca Parales (University of California, USA). *E. coli* BL21 (pET28b_SUMO) containing the AsqJ gene was kindly donated by Profs. Lukas Hintermann and Michael Groll (Technical University of Munich). *E. coli* BL21 (pET22b_H6H) containing the H6H gene was kindly provided by Alejandra B. Cardillo (Universidad de Buenos Aires).

### Culture media

Lysogeny broth (LB) used for cell growth contained: Bacto Tryptone (10 g/L), Bacto Yeast Extract (5 g/L), and sodium chloride (10 g/L). For LB low-salt medium, 5 g/L sodium chloride was used. Agar (15 g/L) was added for solid media. When needed the medium was supplemented with sterile ampicillin sodium salt (0.1 g/L) or kanamycin (0.05 g/L). Mineral Salts Broth (MSB) used for the precultures for the bioreactor cultures contained: $K_2HPO_4$ (16 g/L), $KH_2PO_4$ (14 g/L), $(NH_4)_2SO_4$ (5 g/L), Bacto Yeast Extract (15 g/L); after sterilization the medium was supplemented with sterile glucose (30 g/L), $MgSO_4 \cdot 7H_2O$ (2 g/L) and Kanamycin (0.05 g/L). Bioreactor defined mineral salt medium consisted of: $KH_2PO_4$ (7.5 g/L), citric acid (2.0 g/L), $MgSO_4 \cdot 7H2O$ (5.0 g/L), ferric ammonium citrate (0.3 g/L), 98% $H_2SO_4$ (1.4 mL/L) and trace metal solution (1.5 mL/L). After sterilization, pH is regulated to 6.8 by addition of conc. ammonium hydroxide, followed by supplementation with sterile thiamine hydrochloride (0.3 g/L) and ampicillin sodium salt (0.1 g/L). Trace metal solution contained: citric acid (40 g/L), $MnSO_4 \cdot 2H_2O$ (30 g/L), NaCl (10 g/L), $FeSO_4 \cdot 7H_2O$ (1 g/L), $CoCl_2 \cdot 6H_2O$ (1 g/L), $ZnSO_4 \cdot 7H_2O$ (1 g/L), $CuSO_4 \cdot 5H_2O$ (0.1 g/L), $H_3BO_3$ (0.1 g/L), $NaMoO_4 \cdot 2H_2O$ (0.1 g/L); pH was adjusted to 3.0 with ammonium hydroxide.

### Cloning and vector construction

The pDTG141-Kan expression vector was obtained by replacing the β-lactamase cassette with a kanamycin cassette in pDTG141. The kanamycin resistance gene was amplified from pET28b using the corresponding primers in Table S2 and the resulting amplicon was used in a RFC reaction[32] to switch ampicillin resistance for kanamycin resistance in pDTG141 to give the expression vector pDTG141-Kan. The pKK_CBDO expression vector was constructed by subcloning the CBDO operon from vector pTCB144 into pKK223-3. The CBDO operon was amplified using the corresponding primers in Table S2. The resulting amplicon was digested with *Hind* III and cloned into *Hind* III-digested and CIAP dephosphorylated pKK223-3 to yield pKK_CBDO. The genes encoding for TauD, AlkB and Gab were amplified from *E. coli* genome (DH5α strain) using the corresponding primers in Table S2 followed by digestion with *Xho* I and *Nde* I restriction enzymes and ligation into the *Xho* I/*Nde* I cassette of pET22b (Novagen) to give the expression vectors pET22b_TauD, pET22b_AlkB and pET22b_Gab, respectively. The vector encoding for WelO5 was prepared using a synthetic DNA template (Genscript) with optimized codons for expression in *E. coli*. The WelO5 gene was amplified using the primers in Table S2 and cloned into the XhoI/NdeI cassette of pET22b (Novagen) to give the expression vector pET22b_WelO5. The NDO-derived single-site saturation libraries were prepared by a QuickChange PCR protocol using the corresponding primers in Table S2 and pDTG141 as template. Double and triple mutants were constructed by the same procedure using primers 23–40 and the first-generation mutants as template.

### Protein expression

For the Fe/αKG-dependent oxidases the corresponding recombinant strains of *E. coli* BL21 were grown in LB media (AlkB, Gab, AsqJ, H6H and WelO5) or LB low-salt media (TauD) supplemented with ampicillin (100 mg $L^{-1}$) at 37 °C, 200 rpm. Enzymatic expression was induced with β-D-1-thiogalactopyranoside (IPTG) when the cultures reached $OD_{600} = 0.6$, and incubated under the desired conditions: TauD (0.5 mM IPTG, 30 °C, 5 h),[17b] AlkB (1 mM IPTG, 37 °C, 3 h),[33] Gab (0.5 mM IPTG, 30 °C, 5 h), AsqJ (0.1 mM IPTG, 30 °C, 4 h),[20] H6H (1 mM IPTG, 30 °C, 4 h),[34] WelO5 (1 mM IPTG, 16 °C, 16 h).[22a] Cells were harvested at 4000 rpm for 20 min, resuspended in potassium phosphate buffer (50 mM, pH 7.2) and stored briefly at −4 °C. For the Rieske dioxygenases, the corresponding recombinant strains of *E. coli* JM109 or JM109 (DE3) were grown in LB media supplemented with ampicillin (100 mg $L^{-1}$) at 37 °C, 200 rpm. Enzymatic expression was induced with 0.25 mM β-D-1-thiogalactopyranoside (IPTG) when the cultures reached $OD_{600} = 0.5$, and incubated overnight at 27 °C, 200 rpm. Cells were harvested at 4,000 rpm for 15 min and washed once with potassium phosphate buffer (50 mM, pH 7.2). The cell pellet was resuspended in potassium phosphate buffer (50 mM, pH 7.2) containing 5% v/v glycerol and 5% w/v glucose, frozen and stored at −78 °C. The engineered NDO libraries were expressed in 48-deep-well plates by inoculating single colonies into 4 mL of LB media supplemented with ampicillin (100 mg $L^{-1}$) in each well. Plates were incubated overnight at 37 °C, 180 rpm. 40 μL of these overnight cultures were transferred to a new 48-well plate containing 4 mL fresh LB media containing ampicillin (100 mg $L^{-1}$) and incubated under the same conditions until $OD_{600}$ ~0.6. Enzyme expression was induced by adding 0.25 mM IPTG, following by incubation overnight at 27 °C, 180 rpm. The plates were centrifuged at 4,000 rpm for 30 minutes

and the cell pellets were resuspended in potassium phosphate buffer (50 mM, pH 7.2) containing 5% v/v glycerol and 5% w/v glucose to reach an $OD_{600} = 30$. The cell suspensions were subjected to a freeze/thaw cycle prior to the reactions.

### Whole-cell C–H amination reactions

Reactions using *E. coli* whole cells expressing the non-heme iron oxidases were carried out at 400 μL-scale using $OD_{600} = 30–60$ and 2.5–10 mM substrate concentration in potassium phosphate buffer (50 mM, pH 7.2). In a typical procedure, the whole cell suspensions were transferred to an anaerobic chamber. Additives (αKG, ascorbate, iron salt) were added in the anaerobic chamber from stock solutions in argon purged MilliQ water. Reactions were initiated by addition of substrate (400 mM stock solution in EtOH) and the reaction mixtures were stirred or shaken in the chamber for 12 h at room temperature. After that, the reactions were analyzed by adding 8 μL of internal standard (fluorenone, 50 mM in DMSO), followed by extraction with 400 μL of dichloromethane. The organic layer was removed via evaporation and the residue was dissolved in 300 μL methanol, filtered through 0.22 μm syringe filters, and analyzed by HPLC. Separation method: Injection volume: 20 μL. Flow rate: 1 mL/min. Gradient: 30% acetonitrile in water (0.1% TFA) for 3 min, then increased to 90% over 18 min. Detector: 254 nm. Calibration curves were constructed using synthetically produced products. All measurements were performed at least in duplicate.

### Large scale biotransformation

Scale-up biotransformation was performed in a 5-liter bioreactor (Sartorius Biostat A plus) using a modification of a previously published procedure.[30] Fresh plates of *E. coli* JM109 DE3 (pDTG141-Kan) were used to inoculate 5 mL LB-Kan which was incubated in orbital shaker overnight (150 rpm, 37 °C). Two 500 mL Erlenmeyer flasks containing 150 mL of MSB medium were inoculated with 1.5 mL of the overnight culture and grown for 12 h (37 °C, 150 rpm). Both 500 mL cultures were used to inoculate the bioreactor (Sartorius Biostat A plus) charged with an initial volume of 2.5 L, and set to 500 rpm, 30 °C, and air flow rate of 4 L/min, and a pulse of antifoam agents (Aldrich's Antifoam 201: Silicone dispersion in water 1:1) was added at the beginning of the run. The pH value was adjusted automatically to 6.8 by addition of ammonium hydroxide throughout the reaction. A glucose fed-batch started 6 h after inoculation by adding glucose (0.7 g/mL solution) from an initial rate of 0.08 mL/min to 0.54 mL/min in a 20 h period. Enzyme expression was induced by adding IPTG to a final concentration of 10 mg/L after 12 h from inoculation, and stirrer speed was set to 900 rpm. After the culture reached the stationary phase (~26 h, ~30 g/L cdw), 1.5 L of media was removed from the bioreactor and 1 g of 2,4,6-triisopropylbenzenesulfonyl azide 1a in MeOH was added to a final concentration of 3 mM. Samples were withdrawn at different time points, extracted with DCM, and analyzed by HPLC as described above.

### Statistical analyses

GraphPad Prism software 8 was used for data analysis of Rieske dioxygenase catalyzed reactions. Data are presented as mean ± SD values from five replicates. The results were analyzed and compared by one-way ANOVA followed by Sidak's Multiple Comparison Test, and in all cases statistical significance was set at $P < 0.05$.

## Acknowledgements

*R.F. and V.S. acknowledge financial support from the U.S. National Science Foundation grants CHE-1609550 and CHE-1834390. MS instrumentation was supported by U.S. National Science Foundation grants CHE-0840410 and CHE-0946653. A.V., S.R. and I.C. acknowledge financial support from PEDECIBA, CSIC-UdelaR (Proyect INI-1828), Agencia Nacional de Investigación e Innovación (ANII – Uruguay, Project FCE 103485) and the PhosAgro/UNESCO/IUPAC Partnership in Green Chemistry for Life for a research grant awarded to I.C. A.V. acknowledges CAP-UdelaR for a PhD. Scholarship. We also thank Juan Mauricio Minoia from the Universidad de Buenos Aires for preparing bacterial cultures expressing H6H.*

## Conflict of Interest

The authors declare no conflict of interest.

**Keywords:** non-heme iron-dependent oxidases · Rieske diooxygenases · nitrene transfer · C–H amination · protein engineering

[1] a) B. I. Fedeles, V. Singh, J. C. Delaney, D. Li, J. M. Essigmann, *J. Biol. Chem.* **2015**, *290*, 20734–20742; b) A.-X. Cheng, X.-J. Han, Y.-F. Wu, H.-X. Lou, *Int. J. Mol. Sci.* **2004**, *15*, 1080–1095; c) S.-S. Gao, N. Naowarojna, R. Cheng, X. Liu, P. Liu, *Nat. Prod. Rep.* **2018**, *35*, 792–837; d) H. Nakamura, Y. Matsuda, I. Abe, *Nat. Prod. Rep.* **2018**, *35*, 633–645; e) C. Perry, Emmanuel L. C. De los Santos, L. M. Alkhalaf, G. L. Challis, *Nat. Prod. Rep.* **2018**, *35*, 622–632; f) L. Shen, C.-X. Song, C. He, Y. Zhang, *Annu. Rev. Biochem.* **2014**, *83*, 585–614; g) S. C. Farrow, P. J. Facchini, *Front. Plant Sci.* **2014**, *5*; h) M. D. White, E. Flashman, *Curr. Opin. Chem. Biol.* **2016**, *31*, 126–135; i) M. S. Islam, T. M. Leissing, R. Chowdhury, R. J. Hopkinson, C. J. Schofield, *Annu. Rev. Biochem.* **2018**, *87*, 585–620; j) S. M. Barry, G. L. Challis, *ACS Catal.* **2013**, *3*, 2362–2370.

[2] a) A. L. Feig, S. J. Lippard, *Chem. Rev.* **1994**, *94*, 759–805; b) L. Que, R. Y. N. Ho, *Chem. Rev.* **1996**, *96*, 2607–2624; c) M. Costas, M. P. Mehn, M. P. Jensen, L. Que, *Chem. Rev.* **2004**, *104*, 939–986; d) M. M. Abu-Omar, A. Loaiza, N. Hontzeas, *Chem. Rev.* **2005**, *105*, 2227–2252; e) E. G. Kovaleva, J. D. Lipscomb, *Nat. Chem. Biol.* **2008**, *4*, 186–193; f) S. Martinez, R. P. Hausinger, *J. Biol. Chem.* **2015**, *290*, 20702–20711.

[3] D. J. Ferraro, L. Gakhar, S. Ramaswamy, *Biochem. Biophys. Res. Commun.* **2005**, *338*, 175–190.

[4] a) R. E. Parales, *J. Ind. Microbiol. Biotechnol.* **2003**, *30*, 271–278; b) B. Kauppi, K. Lee, E. Carredano, R. E. Parales, D. T. Gibson, H. Eklund, S. Ramaswamy, *Structure* **1998**, *6*, 571–586.

[5] a) C. Schofield, R. Hausinger, *2-Oxoglutarate-dependent oxygenases*, Royal Society of Chemistry, **2015**; b) F. P. Guengerich, *J. Biol. Chem.* **2015**, *290*, 20700–20701; c) R. P. Hausinger, *Crit. Rev. Biochem. Mol. Biol.* **2004**, *39*, 21–68.

[6] A. Timmins, S. P. De Visser, *Catalysts* **2018**, *8*, 314.

[7] a) W. Hüttel, *Chem. Ing. Tech.* **2013**, *85*, 809–817; b) C. Loenarz, C. J. Schofield, *Nat. Chem. Biol.* **2008**, *4*, 152–156; c) M. Hibi, J. Ogawa, *Appl. Microbiol. Biotechnol.* **2014**, *98*, 3869–3876; d) J. Latham, E. Brandenburger, S. A. Shepherd, B. R. K. Menon, J. Micklefield, *Chem. Rev.* **2018**, *118*, 232–269; e) A. J. Mitchell, J.-K. Weng, *Plant Physiol.* **2019**, *179*, 813–829; f) Y. Nakashima, T. Mori, H. Nakamura, T. Awakawa, S. Hoshino, M. Senda, T. Senda, I. Abe, *Nat. Commun.* **2018**, *9*, 104; g) C. Peters, R. M. Buller, *Catalysts* **2019**, *9*, 221–241.

[8] M. Guo, T. Corona, K. Ray, W. Nam, *ACS Cent. Sci.* **2019**, *5*, 13–28.

[9] a) N. Thevenet, V. de la Sovera, M. A. Vila, N. Veiga, D. Gonzalez, G. Seoane, I. Carrera, *Org. Lett.* **2015**, *17*, 684–687; b) M. A. Vila, M. Pazos, C. Iglesias, N. Veiga, G. Seoane, I. Carrera, *ChemBioChem* **2016**, *17*, 291–295.

[10] M. Davidson, M. McNamee, R. Fan, Y. Guo, W. -c Chang, *J. Am. Chem. Soc.* **2019**, *141*, 3419–3423.
[11] a) S. Giovani, H. Alwaseem, R. Fasan, *ChemCatChem* **2016**, *8*, 2609–2613; b) S. Giovani, R. Singh, R. Fasan, *Chem. Sci.* **2016**, *7*, 234–239.
[12] a) R. Singh, M. Bordeaux, R. Fasan, *ACS Catal.* **2014**, *4*, 546–552; b) R. Singh, J. N. Kolev, P. A. Sutera, R. Fasan, *ACS Catal.* **2015**, *5*, 1685–1691.
[13] M. Bordeaux, R. Singh, R. Fasan, *Bioorg. Med. Chem.* **2014**, *22*, 5697–5704.
[14] a) T. Hudlicky, D. Gonzalez, D. Gibson, *Aldrichimica Acta* **1999**, *32*, 35–62; b) S. E. Lewis, *Chem. Commun.* **2014**, *50*, 2821–2830; c) T. Hudlicky, *ACS Omega* **2018**, *3*, 17326–17340.
[15] a) S. Resnick, K. Lee, D. Gibson, *J. Ind. Microbiol.* **1996**, *17*, 438–457; b) R. E. Parales, K. Lee, S. M. Resnick, H. Jiang, D. J. Lessner, D. T. Gibson, *J. Bacteriol.* **2000**, *182*, 1641–1649; c) C. Chopard, R. Azerad, T. Prangé, *J. Mol. Catal. B* **2008**, *50*, 53–60; d) D. J. Ferraro, A. Okerlund, E. Browna, S. Ramaswamy, *IUCrJ* **2017**, *4*, 648–656.
[16] a) C. Werlen, H.-P. E. Kohler, J. R. van der Meer, *J. Biol. Chem.* **1996**, *271*, 4009–4016; b) S. Yildirim, J. Zezula, T. Hudlicky, B. Witholt, A. Schmid, *Adv. Synth. Catal.* **2004**, *346*, 933–942; c) S. Yildirim, T. T. Franko, R. Wohlgemuth, H.-P. E. Kohler, B. Witholt, A. Schmid, *Adv. Synth. Catal.* **2005**, *347*, 1060–1072.
[17] a) E. Eichhorn, J. R. van der Ploeg, M. A. Kertesz, T. Leisinger, *J. Biol. Chem.* **1997**, *272*, 23031–23036; b) D. Wetzl, J. Bolsinger, B. M. Nestl, B. Hauer, *ChemCatChem* **2016**, *8*, 1361–1366.
[18] a) H. Kondo, Y. Nakabeppu, H. Kataoka, S. Kuhara, S. Kawabata, M. Sekiguchi, *J. Biol. Chem.* **1986**, *261*, 15772–15777; b) P. Ø Falnes, R. F. Johansen, E. Seeberg, *Nature* **2002**, *419*, 178–182.
[19] M. R. Chance, A. R. Bresnick, S. K. Burley, J.-S. Jiang, C. D. Lima, A. Sali, S. C. Almo, J. B. Bonanno, J. A. Buglino, S. Boulton, H. Chen, N. Eswar, G. He, R. Huang, V. Ilyin, L. McMahan, U. Pieper, S. Ray, M. Vidal, L. K. Wang, *Protein Sci.* **2002**, *11*, 723–738.
[20] A. Bräuer, P. Beck, L. Hintermann, M. Groll, *Angew. Chem. Int. Ed.* **2016**, *55*, 422–426; *Angew. Chem.* **2016**, *128*, 432–436.
[21] a) G. Fodor, A. Romeike, G. Janzsó, I. Koczor, *Tetrahedron Lett.* **1959**, *1*, 19–23; b) T. Hashimoto, Y. Yamada, *Plant Physiol.* **1986**, *81*, 619–625; c) T. Hashimoto, Y. Yamada, *Eur. J. Biochem.* **1987**, *164*, 277–285; d) T. Hashimoto, J. Kohno, Y. Yamada, *Plant Physiol.* **1987**, *84*, 144–147; e) T. Hashimoto, J. Kohno, Y. Yamada, *Phytochemistry* **1989**, *28*, 1077–1082; f) J. Matsuda, S. Okabe, T. Hashimoto, Y. Yamada, *J. Biol. Chem.* **1991**, *266*, 9460–9464; g) T. Hashimoto, J. Matsuda, Y. Yamada, *FEBS Lett.* **1993**, *329*, 35–39; h) I. Klinkenberg, A. Blokland, *Neurosci. Biobehav. Rev.* **2010**, *34*, 1307–1350; i) J. Li, M. J. van Belkum, J. C. Vederas, *Bioorg. Med. Chem.* **2012**, *20*, 4356–4363; j) R. Ushimaru, M. W. Ruszczycky, W. -c Chang, F. Yan, Y. -n Liu, H. -w Liu, *J. Am. Chem. Soc.* **2018**, *140*, 7433–7436.
[22] a) M. L. Hillwig, X. Liu, *Nat. Chem. Biol.* **2014**, *10*, 921–923; b) M. L. Hillwig, H. A. Fuhrman, K. Ittiamornkul, T. J. Sevco, D. H. Kwak, X. Liu, *ChemBioChem* **2014**, *15*, 665–669; c) A. J. Mitchell, Q. Zhu, A. O. Maggiolo, N. R. Ananth, M. L. Hillwig, X. Liu, A. K. Boal, *Nat. Chem. Biol.* **2016**, *12*, 636–640.
[23] F. H. Vaillancourt, J. Yin, C. T. Walsh, *Proc. Natl. Acad. Sci. USA* **2005**, *102*, 10111–10116.
[24] J. M. Halder, B. M. Nestl, B. Hauer, *ChemCatChem* **2018**, *10*, 178–182.
[25] M. J. Weissenborn, S. A. Löw, N. Borlinghaus, M. Kuhn, S. Kummer, F. Rami, B. Plietker, B. Hauer, *ChemCatChem* **2016**, *8*, 1636–1640.
[26] a) C. C. Farwell, R. K. Zhang, J. A. McIntosh, T. K. Hyster, F. H. Arnold, *ACS Cent. Sci.* **2015**, *1*, 89–93; b) C. K. Prier, R. J. K. Zhang, A. R. Buller, S. Brinkmann-Chen, F. H. Arnold, *Nat. Chem.* **2017**, *9*, 629–634.
[27] M. T. Reetz, D. Kahakeaw, R. Lohmer, *ChemBioChem* **2008**, *9*, 1797–1804.
[28] B. Kauppi, K. Lee, E. Carredano, R. E. Parales, D. T. Gibson, H. Eklund, S. Ramaswamy, *Structure* **1998**, *6*, 571–586.
[29] D. E. Escalante, K. G. Aukema, L. P. Wackett, A. Aksan, *J. Chem. Inf. Model.* **2017**, *57*, 550–561.
[30] M. A. Vila, M. Brovetto, D. Gamenara, P. Bracco, G. Zinola, G. Seoane, S. Rodríguez, I. Carrera, *J. Mol. Catal. B* **2013**, *96*, 14–20.
[31] N. W. Goldberg, A. M. Knight, R. K. Zhang, F. H. Arnold, *J. Am. Chem. Soc.* **2019**, *141*, 19585–19588.
[32] F. van den Ent, J. Löwe, *J. Biochem. Biophys. Methods* **2006**, *67*, 67–74.
[33] S. Dinglay, S. C. Trewick, T. Lindahl, B. Sedgwick, *Genes Dev.* **2000**, *14*, 2097–2105.
[34] A. B. Cardillo, M. Perassolo, M. Sartuqui, J. Rodríguez Talou, A. M. Giulietti, *Biochem. Eng. J.* **2017**, *125*, 180–189.

Manuscript received: December 26, 2019
Revised manuscript received: February 12, 2020
Accepted manuscript online: March 18, 2020
Version of record online: March 31, 2020